BULLETIN OF THE CHEMICAL SOCIETY OF JAPAN, VOL. 45, 2439—2444 (1972)

Temperature Dependence of Corona-charging Properties on TiO_2-Polymer Dispersion Layers

Takeaki IIDA, Toyokazu NONAKA, and Hiroshi NOZAKI

Institute of Industiral Science, University of Tokyo, Roppongi, Minato-ku, Tokyo, 106

(Received September 3, 1971)

The corona-charging properties of TiO_2-polymer dispersion layers were determined in the dark at temperatures 0°—35°C by the turn-table method. Dispersion layers of TiO_2 (rutile) and polyvinyl acetate, coated on an aluminum foil to about 15 μ thickness, were used. The results showed the rising rate of the surface potential has a maximum at around 20°C. The saturation potential decreases slightly with a rise in temperature. The decay potentials were represented by the plot log V *vs.* $\sqrt{t}$. The relation between log V and $\sqrt{t}$ is linear in certain range of the surface potential, and the gradient increases in proportion to the rise in temperature. This is discussed with the use of an equivalent-circuit model.

Studies have been made on the corona-charging properties of electrophotographic sensors with respect to change with the contents of the photoconductor,[1] sensitization of the corona-charging,[2] and effects of the relative humidity.[3] The results were summarized by Schaffert,[4] Yoshida,[5] and Ionue.[6]

Amick's model for the corona-charging mechanism,[7] and Inoue's empirical equation for the dark decay[8] are often used to explain the behaviors of the corona-charging properties.

Inoue's equation is convenient for representing the experimental results of surface potential decay. The surface potential $V(t)$ at decay period is approximated by the following equation in a certain range of surface potential.

$$V(t) = V_0 e^{-\alpha\sqrt{t}} \quad (1)$$

where V_0 is the initial potential, α is the decay constant, and t is the time from the instant at which corona discharge is turned off. Taking the logarithm of (1), we get

$$\log V(t) = \log V_0 - 0.43\,\alpha\sqrt{t} \quad (2)$$

This means that the decay curve is linear when the log V is plotted against $\sqrt{t}$. According to Inoue's experiments, the gradient depends on such factors as the initial potentials, binder to photocondutcor weight-ratio and amounts of additives.

In this study the corona-charging properties of the sensors were found to depend a great deal on temperature. The results obtained will be of use not only for studying the mechanism of the corona-charging but also for controlling the surface potentials in commercial machines operating at various temperatures.

Experimental

Titanium dioxide of the rutile type was prepared by the hydrolysis of titanium tetrachloride distilled several times, and ignited at 500°C for 2 hrs. The average diameter of the power was about 0.5μ, and the specific surface area as determined by BET was 1.57m²/g. Polyvinyl acetate (PVAc) of the average polymerization degree of 1400 was used as a binder.

Preparation of the dispersion layers was as follows. The ratio of binder to titanium dioxide in weight was chosen to

1) I. Tashiro, T. Kimura, M. Kuwahara, and G. Ohno, *Electrophotography*, **8**, 9 (1969).
2) E. Inoue and T. Yamaguchi, *ibid.*, **5**, 65 (1964).
3) S. Kikuchi, H. Nozaki, and S. Sakata, *ibid.*, **1**, 39 (1959).
4) R. M. Schaffert, "Electrophotography" Focal Press (1965).
5) K. Yochida, "Electrophotography and its Apparatus" Nikkankohgyo (1967).
6) E. Inoue, K. Kikuchi, K. Sayanagi, M. Mori, and S. Wada, "Image Science and Engineering" Kyoritsushuppan (1970), Vols. I, II, III.
7) J. A. Amich, *RCA Rev.*, **20**, 753, 770 (1962).
8) E. Inoue, H. Kokado, T. Yamaguchi, S. Nagashima, and K. Takahashi, *Electrophotography*, **1**, 27 (1962).

be 100/0, 90/10, 70/30, 50/50, 20/80. The materials were mixed in a ball-mill crasher for 10 hr, using ethyl acetate as a solvent. The mixture was coated on an aluminium foil with a film coater, and the samples were dried at 110°C for 2 hr. The thickness of the layers was around 15 μ.

The layers cut out in the size of 12 cm × 7 cm were fixed on an aluminiun plate and kept in a chamber where the relative humidity was kept at 30%—35% for 48hr or more.

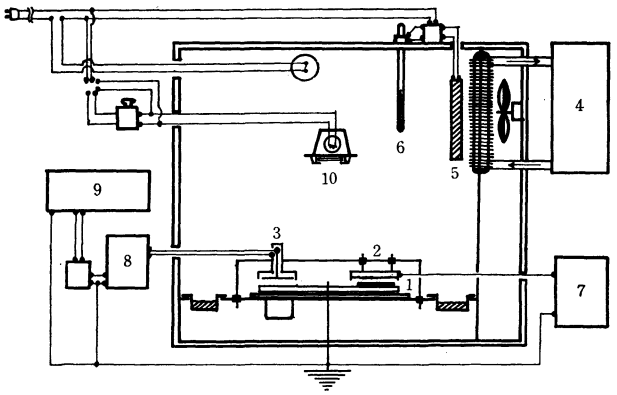

Fig. 1. A schematic illustration of the experimental equipment.
(1) dispersion layer, (2) corona discharger, (3) detecter, (4) refrigerator, (5) cooling fin, (6) relay thermometer, (7) high voltage battery, (8) surface potential meter, (9) recorder, (10) infrared light.

Measurement of the surface potentials at low temperatures was carried out in a chamber where the air was cooled by a cooler to which a cooling medium was circulated from a refrigerator, as shown in Fig. 1. Measurement at high temperatures was carried out with a heater regulated by a relay thermometer. The temperature was raised from 0°C to 35°C by each 5°C. To avoid air leakage from outside, all operations were performed with a pair of rubber gloves attached to the chamber wall.

When the chamber was insulated from the outside, the humidity inside decreased with the rise in temperature. A small amount of humid air was then introduced to the chamber to keep the relative humidity constant at 35%.

The negative corona discharge was carried out by applying −5kV on three steel wands, 0.1mm in diameter, fixed 5mm the turn-table. The corona current was controlled at around 5×10^{-6}A. The turn-table was rotated at 78 rpm. Measurements of the surface potential on the layers were carried out with a surface potential meter of a chopper type.

A typical surface potential change against time is shown in Fig. 2. The slow potential-rise during the initial few seconds is attributed to the charging period of space charges in the layer.[7] After this period, the potential rises almost in proportion to the time from the point M to N in Fig.2, and is saturated to a certain surface potential. The rising rate of the corona potential was determined from the gradient of the line MN. The corona discharge was carried out for one minute, after that the potential gradually decreased to zero. The initial potential V_0 is defined to be the potential at one minute after the turn-off of the corona discharge.

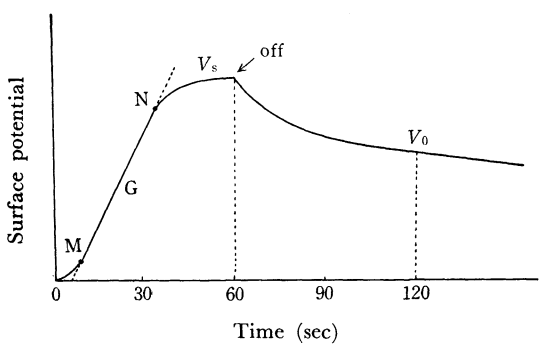

Fig. 2. The typical curve of the surface potential change against the time.

To eliminate the fatigue effect of the corona charging on the layer, an infrared light (200 W) was adjusted to the smaple for 10 minutes at 33°C and the sample was kept in the dark at room temperature for 48 hr between each measurements.

Measurements of the electrical resistivity and the electrocapacity of the dispersion layer were carried out by changing the temperature. A silver electrode (5×5 cm^2) was evaporated in a vacuum on the layer. The specimen was fixed in a dark chamber in which temperature and relative humidity were controlled. A stainless-steel plate was placed on the sample surface with contact pressure 10.0g/cm^2. The electrical resistivity was directly measured with a 610-B Keithley electrometer. The electrostatic capacity was measured with a Wheatstone brige applying an alternative current of 1kHz.

Results

The rising rate of the corona potential G (volt/sec) is plotted against the temperature in Fig. 3. From the results it can be said that G for 0–30% TiO_2-contents increases with a rise in temperature, through its maximum at around 20°C, and suddenly decreases from 25 to 35°C. For 10% and 30% TiO_2-contents, G at 35°C is lower than that at 0°C. However, for 50% and 80% TiO_2-contents, G decreases gradually from 5 to 10°C, becoming almost constant from 10 to 35°C.

The temperature dependence of the asturation potential V_s is shown in Fig.4. The saturation potentials for 0–30% TiO_2-contents are almost constant at 0°–

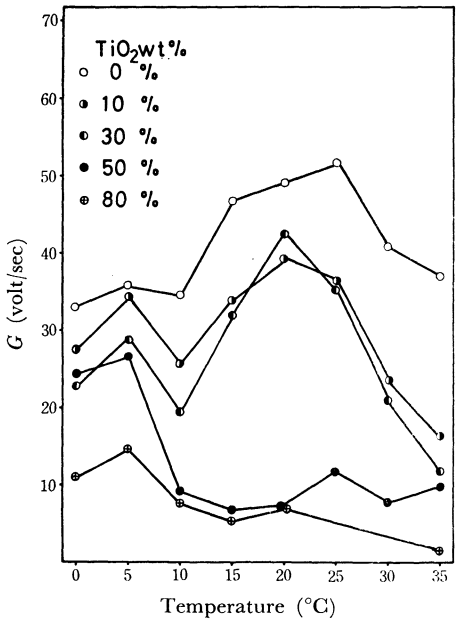

Fig. 3. The rising rate of the surface potential, G (volt/sec), were plotted against the temperature.

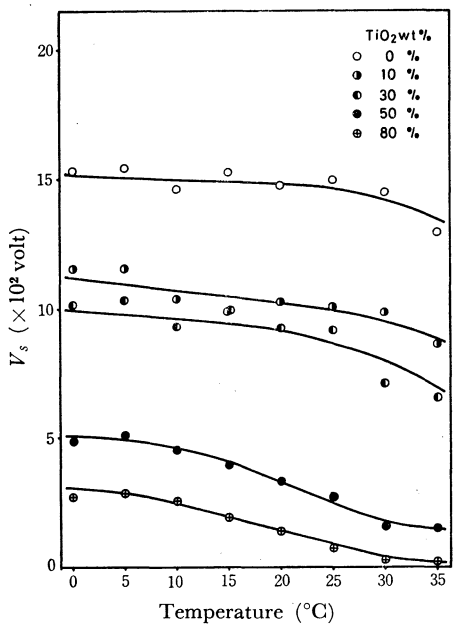

Fig. 4. The temperature dependence of the saturation potential.

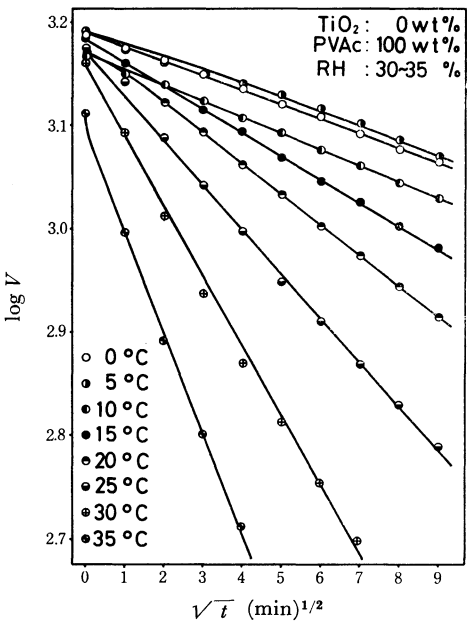

Fig. 6. The logarithm of the dark decay potential on the polyvinyl acetate layer is plotted against the square root of the time at various temperatures.

25°C, decreasing slightly at 25°–35°C. The saturation potentials for 50–80% TiO_2-contents decrease gradually with the rise in temperatures.

The temperature dependence of velocity of the dark-decay is shown in Fig.5. The velocity defined by $(V_s-V_o)/V_s$ increases considerably with the rise in temperature. This tendency is greater for the high percentage of TiO_2-contents.

The dark-decay of the surface potential at various temperatures for long duration was studied by changing the titanium-dioxide contents. The results are represented by the relation between log V and $\sqrt{t}$ in Figs. 6—10.

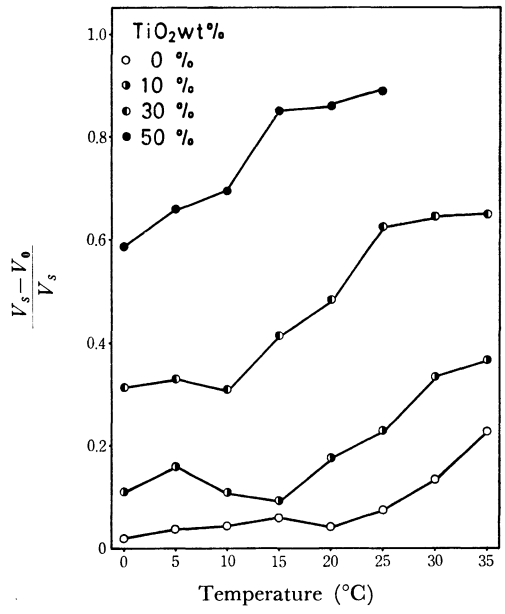

Fig. 5. The temperature dependence of the velocity of the dark decay, where V_0 is the surface potential at one minute after the turn-off of the corona discharge.

A good linear relation is given on the polyvinyl acetate layer for a long duration of the decay (Fig.6). However, the linearity between log V and $\sqrt{t}$ at higher TiO_2-contents does not hold at the initial steps (Figs. 7–8). The decay velocities for 50–80% TiO_2-contents are so rapid that the linearity holds for a short range of the decay period (Figs. 9–10). It can be said that the potential decay increases with the rise in temperature. The temperature dependence of the gradients of the linear lines in the plots between log V and $\sqrt{t}$, *viz.*, the decay constant α, is shown in Fig. 11. The decay

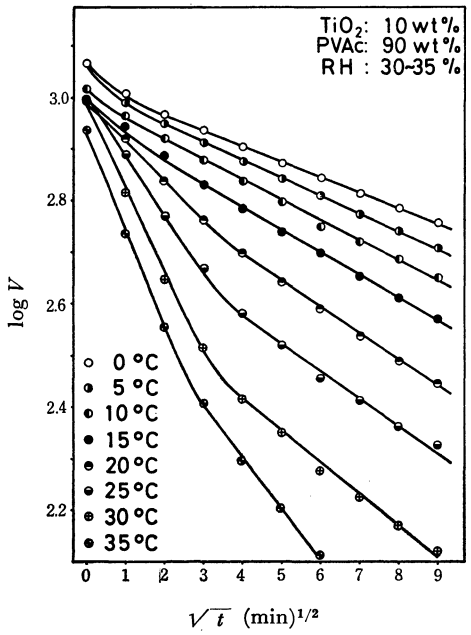

Fig. 7. The logarithm of the dark decay potential on the dispersion layer containing 10 wt% of titanium dioxide is plotted against the square root of the time at various temperatures.

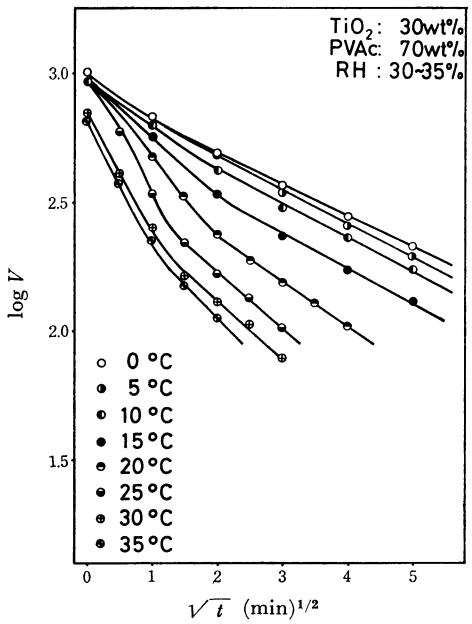

Fig. 8. The logarithm of the dark decay potential on the dispersion layer containing 30 wt% of titanium dioxide is plotted against the square root of the time at various temperatures.

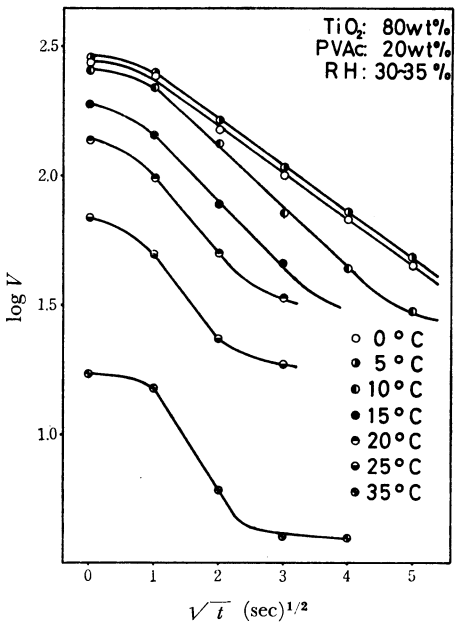

Fig. 10. The logarithm of the dark decay potential on the dispersion layer containing 80 wt% of titanium dioxide is plotted against the square root of the time at various temperatures.

constant increases in proportion to the rise in temperature, and with the increase in the percentage of TiO_2-contents.

The temperature dependence of the air-gap conductivity between the corona and the turn-table at corona-discharging which corresponds to the corona current at the applied voltage of −5kVi sre presented by a dotted line in Fig.12. The solid line represents the resistance of the air gap calculated from the values of the corona current. It can be said that the corona current gradually increases with the rise in temperature.

The resistivity of the layer at various TiO_2-contents is shown as a function of the temperature in Fig.13. The layer of 0% of TiO_2-contents has the highest resistivity, and the resistivity decreases with the increase in TiO_2-contents. In general the resistivity of the layer greatly decreases with the rise in temperature.

The capacitance (per one square centimeter) of the layer at various TiO_2-contents is shown as a funtion of the temperature in Fig.14. The layer of 80% of TiO_2-contents has the highest capacitance, and the capacitance of the layer slightly increases with the rise in temperature.

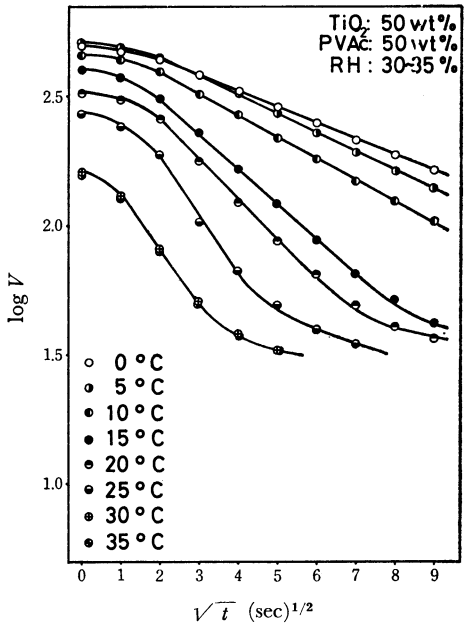

Fig. 9. The logarithm of the dark decay potential on the dispersion layer containing 50 wt% of titanium dioxide is plotted against the square root of the time at various temperatures.

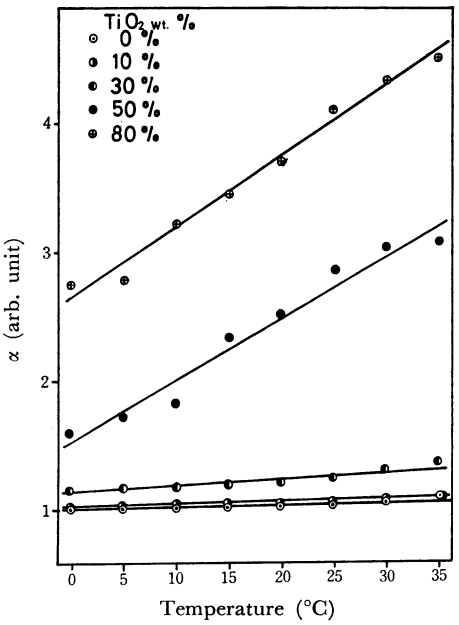

Fig. 11. The temperature dependence of the potential-decay constant, α (in Eq. 2) is shown at various percentage of the titanium-dioxide contents.

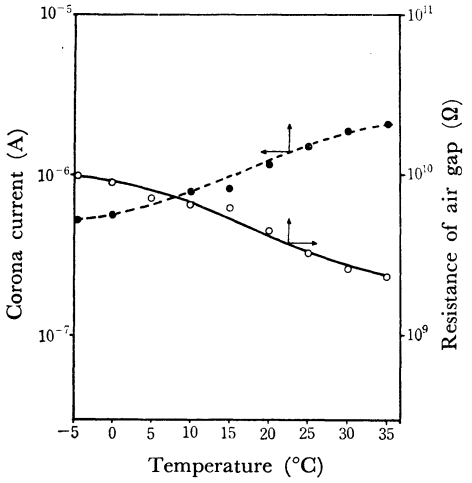

Fig. 12. The dotted line represents the temerature dependence of the corona current, and the solid line represents the resistance of air gap at corona discharging calculated by the corona current.

Discussion

The corona-charging properties of titanium-dioxide dispersion layers were studied by changing the temperature from 0 to 35°C. To interpret the temperature dependence with the use of an equivalent-circuit model shown in Fig.15, the corona current, the resistance of the layer, and the capacitance of the layer were mesaured by changing the temperature. It is reasonable that the corona current (Fig.12) increases with the increase in temperature, since not only the electron emission from the corona electrodes but also the mean free-path of corona ions increase with the rise in temperature. It is also reasonable that the resistivity of the layer decreases with the rise in temperature, since the free electrons in the layer increases with the rise

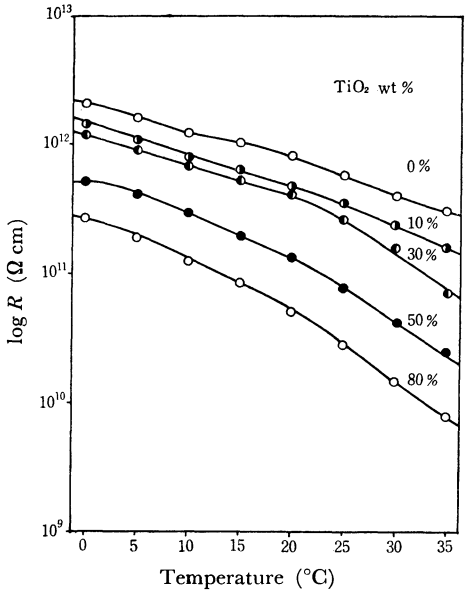

Fig. 13. The temperature dependence of the specific resistivity of the dispersion layer.

9) T. Iida and H. Nozaki, This Bulletin, **42**, 2820 (1969).

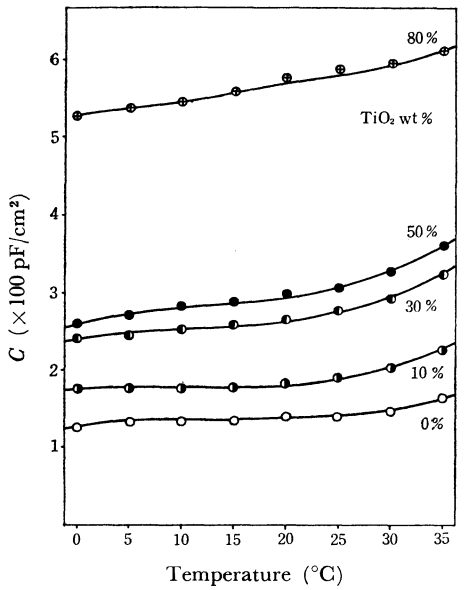

Fig. 14. The temperature dependence of the capacitance of the dispersion layer.

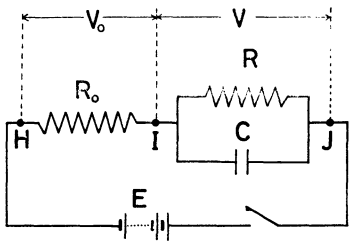

Fig. 15. An equivalent circuit of the dispersion layer.
V_0: Potential difference between H and I
V: Potential difference between I and J
R_0: Resistance of the air gap at corona discharging
R: Resistance of the dispersion layer
C: Capacitance of the dispersion layer

in temperature as shown in Fig.14. Würstlin[10] reported that the dielectric constant of polyvinly acetate increases with a rise from 25°C to 80°C. On the other hand, the dielectric constant of TiO_2-ceramics (rutile) decreases with a rise from 25 to 70°C.[11] In the case of the dispersion layer, the capacitance of the layer increases with a rise in temperature (Fig.14). It can thus be said that the temperature dependence of the capacitance is dominantly governed by the dependence of the dielectric constant of polyvinyl acetate.

In the equivalent-circuit given in Fig.15, when the switch is turned on and a voltage E is applied to the circuit, the change in potential between I and J is given by the equation

$$V = \frac{ER}{R_0+R}\left[1-\exp\left\{-\frac{1}{C}\left(\frac{1}{R_0}+\frac{1}{R}\right)t\right\}\right]. \quad (3)$$

Differentiating V with time, the rising rate of the surface potential is obtained:

$$G = \frac{dV}{dt} = \frac{E}{R_0C}\left[\exp\left\{-\frac{1}{C}\left(\frac{1}{R_0}+\frac{1}{R}\right)t\right\}\right]. \quad (4)$$

10) F. Würstlin, *Kolloid-Z.*, **134**, 143 (1953),
11) L. J. Berberich and M. E. Bell, *J. Appl. Phys.*, **11**, 681 (1940).

Since G is a function of three independent variables of R_0, R, and C, we can not satisfactorily explain the temperature dependence of G only by means of the partial differentiation of G with R_0, R, or C. We thus calculated G directly with the use of the observed values of R_0, R, and C. The rising rate of the surface potential calculated by Eq. (4), in which time was taken at ten seconds, with the use of the data, R_0, R, and C in Figs.12—14, is shown in Fig.16. It can be said that G for 0% TiO_2-contents has a maximum at around 25°C, and the maximum shifts to lower temperature range with the increase in TiO_2-contents. Consequently, G for 80% TiO_2-contents has a maxiumm at around 10°C. The agreement between the calculated values and the observed values (Fig.3) is fairly good.

The saturation potential is given by $ER/(R_0+R)$ from Eq. (3). Figure 4 shows that V_s depends on the temperature of the layer. V_s was calculated with the use of the data R_0 and R in Figs. 12—13 as a function of temperature. In this case the agreement between the calculated values and the observed values (Fig. 4) is also fairly good.

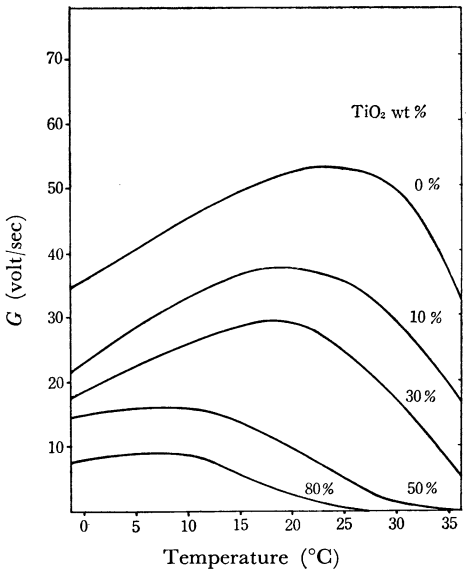

Fig. 16. The rising rate of the surface potential calculated by the equation (4) with the use of the data, R_0, R, and C in Figs. 12—14.

In the case of the discharging process, when the switch is turned off, the discharging current flows only through the resistance of the layer. Therefore, the speed of the dark decay depends greatly on the resistance of the layer. Figure 5 shows that the velocity of the dark decay depends greatly on the temperature of the layer, since R of the layer decreases with a rise in temperature (Fig.13)

The results in Figs.6—10 show that the logarithm of the decay potential decreases in proportion to the square root of the time at a certain range of the decay period. It is not possible to derive directly such a relation with the use of the simple qeuivalent-circuit shown in Fig. 15. Inoue[8] and Papazian[12] proposed a more complex empirical equation in which the summation of the exponential terms of $V_i \exp(-t_i/R_iC_i)$ is considered, where V_i, R_i, and C_i are the potential, resistance and capacitance at the time t_i, respectively. However, it is rather difficult to calculate the potential decay with the use of V_i, R_i, and C_i, since R_i and C_i are not easily measured in actual cases.

We should point out that the decay constant α increases in proportion to the temperature rise from 0° to 35°C. It is not possible to derive such a relation with the use of the simple equivalent-circuit model shown in Fig.15. A more complex model will be needed.

The authors wish to thank Mr. T. Watabe, Mr. H. Ishii, and Mr. T. Takayama for their experimental assistance in this work.

12) H. A. Papazian, P. A. Flinn, and D. Trivich, *J. Electrochem. Soc.*, **104**, 84 (1957).